Inorganic Sensing Using Organofunctional Sol–Gel Materials

NATHAN A. CARRINGTON AND ZI-LING XUE*

Department of Chemistry, The University of Tennessee, Knoxville, Tennessee 37996-1600

ABSTRACT

This Account describes recent work in the development and applications of sol–gel sensors for concentrated strong acids and bases and metal ions. The use of sol–gel films doped with organic indicators for the optical sensing of concentrated strong acids (HCl, 1–10 M) and bases (NaOH, 1–10 M) has been explored, and the development of dual optical sensor approaches for ternary systems (HCl–salt–H_2O and NaOH–alcohol–H_2O) to give acid and salt, as well as base and alcohol, concentrations is discussed. The preparation of transparent, ligand-grafted sol–gel monoliths is also described, and their use in the analysis of both metal cations (Cu^{2+}) and metal anions [Cr(VI)] is presented. A new model using both metal ion diffusion and immobilization by the ligands in such monoliths has been developed to give metal concentrations using the optical monolith sensors. In addition to optical sensing, a method utilizing ligand-grafted sol–gel films for analyte preconcentration in the electrochemical determination of Cr(VI) has been explored and is discussed.

1. Introduction

First reported some 150 years ago, the sol–gel process refers to a multitude of reactions using alkoxide precursors to prepare solid products such as glasses and ceramic oxides.[1–3] In this process, an alkoxide precursor, such as $Si(OR)_4$, is hydrolyzed. The resulting silanols undergo condensation to form a cross-linked inorganic matrix and a three-dimensional porous glass. These sol–gel reactions, summarized in Scheme 1, are profoundly affected by many factors, such as the size of the alkoxide ligand,

Nathan A. Carrington was born in Pittsburgh, PA, in April 1981. He graduated from Erskine College in 2003 with a B.S. in Chemistry. He is currently carrying out his Ph.D. research at the University of Tennessee with Zi-Ling (Ben) Xue. His research is focused on novel electrochemical and optical sensing techniques.

Zi-Ling (Ben) Xue was born in Wuxi, Jiangsu, China, in December 1959 and grew up in Nanjing. He studied physical chemistry–catalysis at Nanjing University–Nanjing College of Pharmacy, and received his B.S. degree in 1982. He was selected in 1983 as a Chemistry Graduate Program (CGP or William von E. Doering Program) fellow and entered the Ph.D. program at the University of California at Los Angeles in 1984, studying organometallic chemistry with Herbert D. Kaesz. After receiving his Ph.D. degree in 1989, he moved to Indiana University in 1990 as a postdoctoral fellow with Kenneth G. Caulton and Malcolm H. Chisholm and in 1992 accepted a position as Assistant Professor at the University of Tennessee. He was promoted to Associate Professor in 1997 and Professor in 2001 and is now a Paul and Wilma Ziegler Professor of Chemistry. He served in 1999–2001 as a member of the Executive Committee, ACS Division of Inorganic Chemistry, and is now the division Membership Committee Chair. Professor Xue has received several awards including a National Science Foundation Young Investigator Award, Camille Dreyfus Teacher–Scholar Award, DuPont Young Professor Award, Changjiang Lecture Professor, Distinguished Oversea Young Scholar Award (Chinese Natural Science Foundation), and UK Royal Society Kan Tong Po Visiting Professorship. His early interests in metal-based catalysis led to his current work in synthetic and analytical inorganic chemistry.

Scheme 1. A Summary of the Basic Sol–Gel Reactions

solution pH, types and concentrations of solvents, temperature, and catalysts.[1–5] By carefully tailoring these variables, sol–gel materials have been produced for numerous applications, including electronics, optics, separation technology, catalysis, and sensing.[1,6]

There are many properties of sol–gels that make them particularly attractive for sensing applications. Sol–gels are compatible with numerous chemical agents, making possible the incorporation of sensing elements onto sol–gel substrates. Since little or no heating is required during the sol–gel process, thermally sensitive organic molecules have been encapsulated within the gel interiors.[7] This encapsulation is usually accomplished using either doping or grafting processes to give organofunctional sol–gel materials. Doping involves the physical entrapment of a reagent inside the substrate, while grafting involves the anchoring of a reagent through covalent bonding.[7–9] Doping techniques are simple and applicable to many organic compounds, but the pore size must be carefully tailored because dopant leaching is often a problem. Grafting techniques yield highly reproducible, stable products, but the overall process can be tedious. The reagents need to contain a $-Si(OR)_3$ group, and this limits the selection of reagents suitable for the grafting processes. The porous nature of sol–gels allows for the delivery of analytes to the encapsulated reagent, resulting in the interactions required for sensing applications. Sol–gels have found particular use in optical sensing, because they are transparent in the visible region.[10] Such sensors have been developed for monitoring pH,[2,4,8,11–13] metal ions,[14,15] and a variety of other analytes.[16] Sol–gels have also been used in electrochemical[17–21] and spectroelectrochemical[22] sensing applications. The depth and breadth with which sol–gels have been used in chemical sensing expands over a large area.[3,6,9,10,16a,16b,16c,16d,20]

In this Account, we present research involving new sol–gel approaches to inorganic sensing. Trained as an inorganic/organometallic chemist, one of the authors (Z.X.) started his independent academic career in 1992 by studying synthetic and mechanistic chemistry of metal–Si-bonded complexes.[23] The Measurement and Control Engineering Center at the University of Tennessee and its member companies were interested in developing on-line sensors for concentrated strong acids (e.g., 1–11 M HCl) and bases (1–10 M NaOH). We investigated SiO_2-based optical sensors for these widely used inorganic chemicals and thus started our research in sol–gel chemistry. Strong acids and bases are often used in the presence of other chemicals such as salts and mixed solvents in industry.

* Corresponding author. E-mail: xue@utk.edu.

The ionic strength of these solutions contributes significantly to sensor response. We subsequently investigated dual sol–gel sensor approaches to ternary systems. Our more recent studies include metal ion sensing by monolith optical sensors and sol–gel-based electrochemical processes. Our work in the development of new inorganic sensing methods is described. We hope this research demonstrates the unique ways in which sol–gels are employed for a multidisciplinary approach to inorganic sensing.

2. Optical Sensors for Concentrated Strong Acids and Bases

Concentrated strong acids and bases, such as HCl and NaOH, are among the largest volume chemicals manufactured in the world and are widely used in many industrial processes such as the production of paper and pulp, soap and detergents, oil, and textiles.[24,25] Few rapid, reliable methods have been developed, however, for their on-line determination, although many pH sensors have been developed. In our recent work, optical sensors have been developed for high-acidity ([H^+] = 1–11 M) and high-basicity ([OH^-] = 1–10 M) measurements.[2] The technique of doping indicators in sol–gel thin films had been successfully used to make pH sensors (usually for the pH 3–12 range).[5,8,10b] The acid or base concentrations here are, however, outside the normal pH range of 1–14. The development of the sensors relies on the following: (1) selection of *stable* acid and base indicators with equilibria in the acidity and basicity ranges; (2) preparation of indicator-doped sol–gel matrices that resist acid or base attack in the highly corrosive acid and basic environments— this was especially challenging in 1–10 M NaOH solutions; (3) control of pore sizes so that the indicator molecules do not leach out while allowing quick H^+ and OH^- diffusion through the sensor films to yield fast responses (1 and 5 s for acid and base sensors, respectively), a key to the success of the sensors. Once the thin-film sensors were prepared, these doped indicators gave responses related to acid and base concentrations and were monitored using visible spectroscopy. The sensor films were kept dry until use.

Several dyes were doped in sol–gel films as acid sensors. Bromocresol purple (BCP) was chosen first as an indicator due to its high stability in concentrated HCl and its resistivity to oxidation.[26] This dye was mixed with Si(OMe)$_4$ in a solution of H$_2$O, MeOH, and cetyltrimethylammonium bromide (CTAB) containing HCl as catalyst and was coated onto a glass surface to give a thin film of 2.7(0.4) μm thickness. Acid and base catalysts were found to give sensor films of different morphologies and properties. Scanning Electron Microscopy (SEM) images revealed that base-catalyzed hydrolysis produced condensed particulate sols, while acid-catalyzed hydrolysis gave more branched polymeric sols. Figure 1 shows spectra for a BCP-doped sensor film in HCl solutions that give a nonlinear calibration plot. Figure 2 demonstrates the reversibility of these acid sensors. One BCP acid sensor
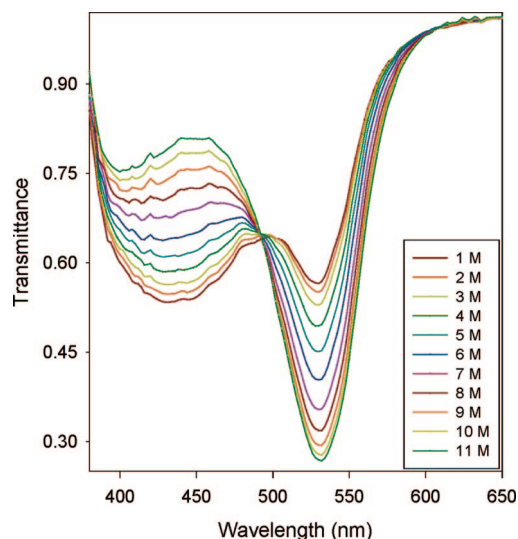

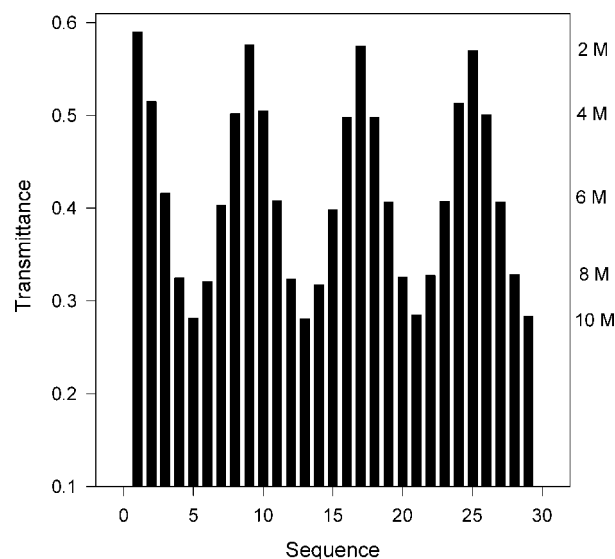**FIGURE 1.** Typical transmission spectra of a BCP-doped sensor film in HCl solutions.

FIGURE 2. Response reversibility of a BCP-doped sensor film. The averages of the response in the range of 546–550 nm are shown.

was placed in 6 M HCl for 9 months except during tests every 2 weeks in 0, 2, 6, and 10 M HCl in both the incremental and decremental directions. A standard deviation of 2% was observed with one initial calibration, showing that the sensor was robust and durable. Recently, Shamsipur,[12a] Wang[12b] and co-workers have also reported high-acidity determination using indicator-doped sol–gels.

The isoelectric point of silica sol–gel is close to pH 2.[2a] Thus, the sensor is vastly protonated in 1–11 M HCl. The diffusion of hydronium ions through the positively charged sol–gel surface during our acidity measurements is slower than that through a neutral sol–gel surface, possibly contributing to the reduction in response time.

The process to form base sensors is similar to that used to prepare the acid sensors, with a few notable differences. First, there are fewer indicator dyes with an appropriate pK_a (13–18) and chemical stability to OH^- attack and oxidation by air. Secondly, SiO$_2$/ZrO$_2$-polymer composites were used as sensor materials to give films of 4.1(0.4) μm
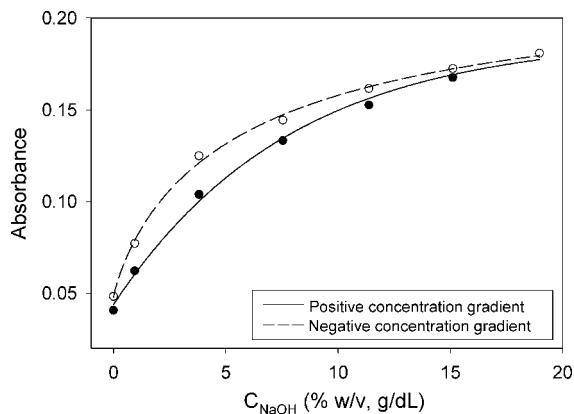
FIGURE 3. Hysteresis profile of a thiazole yellow GGM sensor (ZrO_2/SiO_2–PSMMA film) in NaOH solutions.

FIGURE 4. Responses of a BCP-doped sensor in $CaCl_2$–HCl solutions.

thickness. SiO_2 itself is consumed in concentrated base. SiO_2/MO_2 was found to be stable in highly caustic media,[27] and SiO_2/ZrO_2 showed the best performance as a sensor support. In addition, polymers were incorporated, poly(styrene methyl methacrylate) (PSMMA) to enhance the film strength and reduce indicator leaching, and ionic Nafion to enhance OH^- diffusion and sensor response. Without Nafion, SiO_2/ZrO_2 films showed response times of several hours. The response times dropped to 50 s for SiO_2/ZrO_2–PSMMA films, 15 s for SiO_2/ZrO_2–Nafion–PSMMA films, and 5 s for SiO_2/ZrO_2–Nafion films. A large organic polymer content (>80 wt % of the precursors), however, resulted in less transparent films that peeled off easily. Brunauer–Emmett–Teller (BET) analyses of bulk SiO_2/ZrO_2 showed an average pore size of ca. 40 Å with a surface area of ca. 310 m^2/g. The responses of the base sensors in 1–10 M NaOH are similar to those of acid sensors (Figures 1 and 2). A 30-day durability test, during which the sensors were kept in 4 M NaOH except when they were exposed to 8 M NaOH for measurements, showed a standard deviation of <4%.[2b]

Hysteresis of the sensors and its contributions to the error of measurement, a critical factor in many optical sensors, were also investigated.[2c,13b] The analyte diffusion process can have a profound effect on the reversibility of the sensing scheme. When a sensor is placed in an analyte solution, a concentration gradient develops and the transport of the analyte through the sensor is controlled by this gradient. If the analyte concentration in the exterior solution is larger than that inside the sensor, a positive concentration gradient is established and the analyte diffuses into the sensor. Conversely, if the concentration in the exterior solution is smaller than that inside the sensor, a negative gradient develops, and the analyte diffuses out of the sensor. Figure 3 shows the responses of a base sensor under negative and positive NaOH gradients. The absorbencies under a negative gradient were larger than those at the same concentrations under a positive gradient. This small but observable hysteresis indicates that when the external base concentration is decreased, it takes longer for the OH^- ions to diffuse out of the films. These diffusion rate differences likely reflect the ability of the s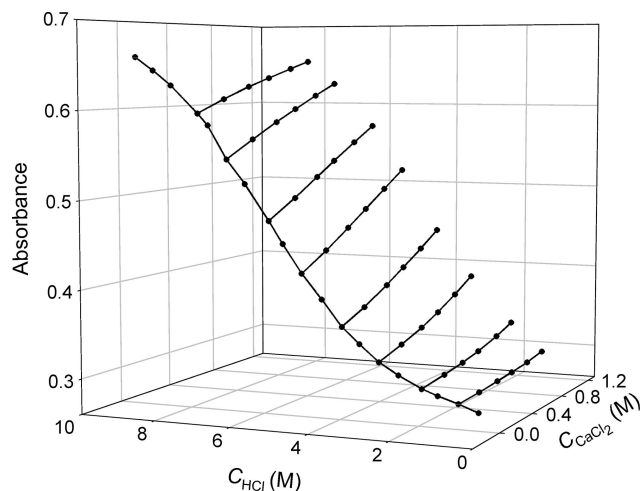olution to transfer OH^- to and from the sensor support. However, by carefully controlling the composition of these acid and base sensors, one can keep hysteresis to a minimum.

3. Dual-Sensor Approaches to Ternary Systems

Concentrated strong acids and bases are commonly used in industry in the presence of other chemicals such as salts in acidic pickling solutions and aqueous–organic mixed solvents in basic pulp bleaching processes.[24,25] The addition of these species results in large changes in ionic strength of the solutions. For optical sensors using indicator equilibria as the transducing mechanism, responses are greatly affected by these changes, shifting the indicator equilibrium. In other words, both the acid and salt contribute to the sensor response in an acid–salt–water ternary solution, and the indicator absorbance, *A*, is an *unknown* function of the two variables, concentrations of the acid (C_{acid}) and salt (C_{salt}). A similar case was observed for base in mixed water–alcohol solutions. The salt and alcohol contributions lead to large analytical errors, sometimes as large as 99%. After the sensors for concentrated acids and bases had been developed, we focused our attention on new dual-sensor approaches for measuring C_{acid} and C_{salt} in salt-containing acidic solutions,[11] as well as C_{base} and $C_{alcohol}$ concentrations in basic mixed solvent systems.[13]

In the acid sensor studies, LiCl, $CaCl_2$, and $AlCl_3$ were used to give solutions of varying ionic strength. By monitoring the absorbances, *A* and A^0, of two *independent* transducers in salt-containing and salt-free acidic solutions, respectively, it was found that the slope of *A* vs C_{salt} at a given acid concentration, $(\partial A/\partial C_{salt})_{C_{acid}}$, is proportional to the respective tangent of the A^0 vs C_{acid} plot for a salt-free acid solution, $(dA^0/dC_{acid})_{C_{salt}=0}$ (eq 1). Figure 4 demonstrates this relationship.

$$(\partial A/\partial C_{salt})_{C_{acid}} = \beta(dA^0/dC_{acid})_{C_{salt}=0} \quad (1)$$

From this relationship, the C_{acid} and C_{salt} contributions were resolved for each of the two transducers (indicators).

In other words, this relationship led to two independent analytical functions, $A_1 = f_1(C_{acid}, C_{salt})$ and $A_2 = f_2(C_{acid}, C_{salt})$, for the two transducers and, through further work, two independent equations in eqs 2 and 3 containing the two variables (C_{acid} and C_{salt}).[11a] Two separate measurements with the two transducers then determined C_{acid} and C_{salt} of the salt-containing acid solution.

$$A_1 = f_1(C_{acid}) + \beta_1 f_1'(C_{acid}) C_{salt} \qquad (2)$$

$$A_2 = f_2(C_{acid}) + \beta_2 f_2'(C_{acid}) C_{salt} \qquad (3)$$

Using these equations from the dual transducer approach, errors in C_{acid} measurements dropped significantly (24% to <2% for LiCl–HCl, 60% to <4% for CaCl$_2$–HCl, and 43% to <1% for AlCl$_3$–HCl solutions). Furthermore, this approach provided greater accuracy in C_{salt} determination for more concentrated salt solutions.

A similar dual-transducer approach was carried out involving the base sensors in which total sensor absorbance (A) was found to be a function of both base and alcohol concentrations. A linear relationship (eq 4) was obtained, resulting in the derivation of two independent equations (eqs 5 and 6) when using two independent transducers.

$$(\partial A / \partial C_{alcohol})_{C_{base}} = d C_{base} + e \qquad (4)$$

$$A_1 = c_1 + a_1 \ln(C_{base} - b_1) + (e_1 + d_1 C_{base}) C_{alcohol} \quad (5)$$

$$A_2 = c_2 + a_2 \ln(C_{base} - b_2) + (e_2 + d_2 C_{base}) C_{alcohol} \quad (6)$$

Using this approach, C_{base} and $C_{alcohol}$ could be determined, reducing errors in the C_{base} determination in mixed methanol and ethanol solutions from as much as 95% to <10% in most cases. Measurements in isopropanol solutions gave larger errors than those in methanol and ethanol, likely due to the lower polarity of isopropanol relative to these other organic solvents studied.

4. Monolith Metal Ion Optical Sensors

Metal compounds constitute a large class of inorganic species, and they are widely used in many industries. Although there are several well-established, conventional techniques for their determination, such as atomic absorption spectroscopy (AAS) and inductively coupled plasma mass spectroscopy (ICP-MS), it is often necessary to make field measurements that cannot be conducted in a laboratory. The development of sensors to monitor metal ion concentrations in both industrial and environmental settings is an emerging and challenging field. Many metal ion sensors that have been developed rely on electrochemical methods for determination,[28] although some optical methods have been reported.[15b] After our work in sol–gel thin films for concentrated strong acids and bases, we turned our attention to metal ion sensing using sol–gel monoliths.[14]

Monoliths are attractive for use in sensing applications due to their highly porous nature and their longer sensor path length than that in thin films. The pores allow the grafting of bulky organic functional groups to the sol–gel backbone, and reagent leaching is not expected since the

Scheme 2. Preparation of the blank and amine-grafted sol–gel monoliths.
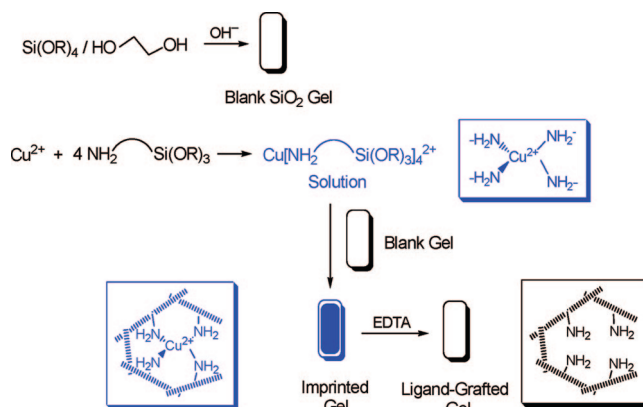
functional groups are chemically bound to the gel interior, unlike the encapsulated dyes in the acid and base sensors. Unlike organic dyes used in acid and base sensing, two features of metal–ligand complexes limit their use in metal ion sensing: (1) metal complexes usually have smaller molar absorptivities than acid and base indicators, and a thin film with a short sensor path length is thus usually not suitable for metal ion sensing; (2) the overall equilibria of complex formation ($M^{m+} + nL \rightleftharpoons ML_n^{m+}$) are usually exclusively shifted to the complexes, and the equilibrium and stability constants are thus exceedingly large. In the case of Cu(NH$_2$Et)$_4^{2+}$, for example, $K = 3.2 \times 10^{10}$. In addition, the metal–ligand complexation reactions such as those between Cu^{2+} and amines are normally very fast. As a result, ligands are quickly saturated, making it difficult to conduct quantitative analysis based on metal–ligand complexation. In other words, the equilibria are in general not sensitive to change in metal concentration. We developed a two-prong approach to address these two features that limit the use of metal–ligand complexation in metal ion sensing: (1) monoliths as sensor materials because they provide a longer sensor path length than thin films, allowing for the detection of metal–ligand complexes with small molar absorptivities; (2) a combination of metal ion diffusion inside a monolith to the binding sites and subsequent metal complexation with ligands grafted on the monolith—A mathematical model has been developed to characterize this process, giving quantitative analyses of the metal ions.

The preparation of such crack-free, optically transparent sol–gel monoliths with mesosized pores was, however, a difficult task.[14b] Scheme 2 illustrates the procedure in the preparation of blank and amine imprint-grafted monoliths. Blank monoliths were synthesized through the hydrolysis of Si(OMe)$_4$ in the presence of ethylene glycol, a porogen. The use of ethylene glycol is an important factor here, because it leads to mesopores in the gel. Once the blank monoliths were formed, they were imprint-grafted by immersion in solutions of Cu[H$_2$N–(CH$_2$)$_3$–Si(OMe)$_3$]$_4^{2+}$. This complex diffused into and was grafted onto the monoliths, resulting in colorless supernatants and blue, transparent gels. The monoliths were then washed stepwise with pure, 75%, 50%, and 25% MeOH,

and finally water. This gradual washing procedure helped reduce surface tension and prevented gel cracking when a monolith prepared in the organic solvent methanol was then placed in water. Removing a monolith from methanol and placing it directly in water often resulted in cracking of the gel. Once the monoliths had been exposed to water, the Cu^{2+} ions were then removed by washing the gels in aqueous ethylenediamine tetraacetate (EDTA) solutions, because EDTA has a higher binding affinity for Cu^{2+} ions than the amine ligands in the monoliths.[14a] When the gels again appeared colorless, they were washed with water and allowed to age. Unlike the thin films discussed in the previous sections, it was necessary that these monoliths remain wet to prevent their cracking and breaking. Such durable, transparent sol–gel monoliths are rare.[14b]

BET measurements showed that the blank monoliths were mesoporous (pore diameter of ca. 47 Å). SEM images of the monoliths showed a packed network of spherical particles, indicative of a base-catalyzed sol–gel process in which colloidal silica clusters are initially formed and then linked together through gelation. When the amine-functionalized monoliths are exposed to an aqueous Cu^{2+} solution, they remove Cu^{2+} ions from solution, forming blue Cu^{2+}–amine complex(es).[14a,14b]

Using these amine-grafted monoliths for Cu^{2+} sensing, we developed a new mathematical model for the diffusion of an "unlimited" supply of Cu^{2+} ions and their subsequent immobilization in the monolith. This model unifies two fundamental kinetic processes during the metal sensing with the amine-grafted monoliths: (1) metal ion diffusion to the binding sites; (2) metal–ligand (ML_n) complexation. Slow metal ion diffusion is followed by a fast immobilization reaction with the ligands (especially for Cu^{2+} and amines, for example, because they are known to have large rate constants of reactions)[29] to give a complex(es). Inside the region where the ligands have been saturated, the diffusion of the metal ions reaches a steady state with a constant external Cu^{2+} concentration (C_0). Thus, if the complex(es) could be observed spectroscopically, the absorbance of the product, A_p, is described in eq 7.

$$A_p = 2\sqrt{2}\varepsilon_p(L_0C_0Dt)^{1/2} \qquad (7)$$

where ε_p = molar extinction coefficient of the complex, L_0 = concentration of the ligands in the monolith, D = diffusion constant of the metal ions inside the monolith, and t = time.[14a]

Following this mathematical model, the monolith was housed in a Teflon cell and monitored by optical-fiber visible spectroscopy as an aqueous $CuCl_2$ solution was pumped through. Absorbance (A_p) vs $t^{1/2}$ plots for Cu^{2+} concentrations (200–800 mM) were linear (correlation coefficient $R = 0.999$), suggesting that the Cu^{2+} diffusion and immobilization in the amine-functionalized monoliths occur by the model in eq 7. In addition, the Cu^{2+} diffusion constant D is similar to a reported value,[14a] providing further evidence of the accuracy of the model. 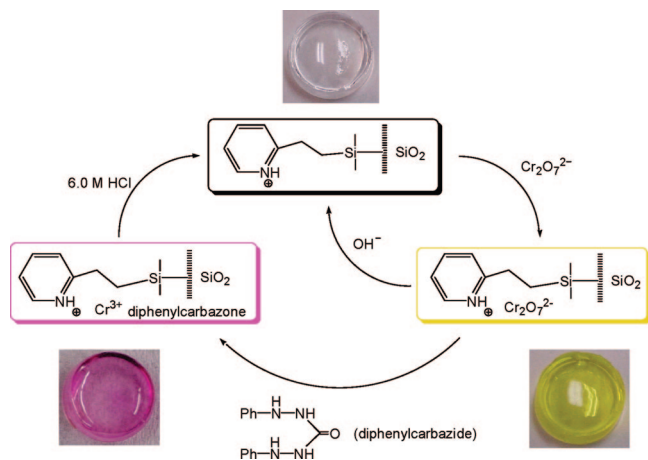This model may be used in other chemical sensors that depend on slow analyte diffusion followed by fast immobilizing reactions.

It should be pointed out that the quantitative determination of Cu^{2+} ions here using amine-functionalized sol–gel monoliths relies on the formation of Cu^{2+}–amine complexes within the sol–gel matrix and the diffusion of Cu^{2+} ions inside the monoliths. This represents one new optical method of metal ion sensing. Of course, many metal ions exist as positively charged *cations*, and they form complexes with ligands that often have characteristic UV–visible spectra. Thus, the new method here may be potentially used in the sensing and quantification of other metal cations. Another class of metal ions, especially those at high oxidation states, exist as oxo *anions*. This class of metal ions includes chromate ($HCrO_4^-$, CrO_4^{2-}), dichromate $Cr_2O_7^{2-}$, permanganate MnO_4^-, and polyoxometalates. These oxo anions are in fact complexes between metal cations and oxo ligands, and they often have unique UV–visible spectra. The oxo ligands form a tight coordination sphere around the metal ions, making it difficult for other ligands to bind to them. In other words, the method that we developed for *cationic* metal ion (Cu^{2+}) sensing is not effective for *anionic* metal ions, and we thus recently investigated a new approach for the sensing of anionic metal ions.

Of particular interest to us is the sensing of Cr(VI) chromate, because it is a suspected carcinogenic agent and toxic pollutant even at trace levels. Several processes had been reported for the quantification of Cr(VI) in solution, including spectroscopic methods,[15a] mass-sensitive devices,[30] and electrochemical detection.[31] We investigated the use of sol–gel monoliths for Cr(VI) quantification at both the ppm and ppb levels. Pyridine-functionalized monoliths for Cr(VI) sensing were prepared by a method similar to that used in the preparation of amine-functionalized sol–gel monoliths for Cu^{2+} sensing (Scheme 2).[14c] These monoliths rely on the Cr(VI) preconcentration inside the gels due to the electrostatic interaction between the positively-charged pyridinium groups in the monolith and the negatively-charged Cr(VI) anions in solution. For the ppm-level Cr(VI) solutions, the monoliths exhibit a yellow color change characteristic of Cr(VI) uptake, and this is measured by visible spectroscopy. Cr(VI) concentrations at the ppb level are below the detection limit by the direct spectroscopic measurement. However, by addition of diphenylcarbazide [PhNH–NH–C(=O)–NH–NHPh], a well-known reagent that reduces Cr(VI) to Cr(III) and produces a magenta-colored complex,[15a] to monoliths previously exposed to ppb-level Cr(VI) solutions, a distinct color change occurs within the gels that is measured by visible spectroscopy. With use of this method for Cr(VI) determination, concentrations as low as 10 ppb could be measured, and environmental samples spiked with Cr(VI) could be accurately measured despite the presence of intereferences.

Scheme 3 illustrates the overall cycle for the Cr(VI) sensing process using these monoliths. The monolith shown is either partially regenerated through exposure to a NaOH solution or completely regenerated through

Scheme 3. Sensing cycle for the Cr(VI) monolith system. Reprinted from ref 14c, Copyright 2007, with permission from Elsevier.

FIGURE 5. Square-wave voltammograms of various Cr(VI) solutions collected at a pyridine-functionalized sol–gel electrode. Reprinted from ref 21a, Copyright 2006, with permission from Elsevier.

exposure to diphenylcarbazide and HCl. Monoliths treated in this manner were found to show reproducible Cr(VI) uptake and sensing from cycle to cycle, making these pyridine-functionalized sol–gels some of the only regenerable optical sensors capable of determining Cr(VI) at the ppb level.

5. Sol–Gel-Based Electrochemistry

Our work described thus far involves optical sensing by sol–gel materials. We recently studied sol–gels and electrochemical sensing of metal ions.[21] Many research groups have conducted studies using sol–gel modified electrodes for the enhanced determination of various analytes.[16d,20] A majority of these techniques have used spin-coating to deposit functionalized sol–gels on electrode surfaces. Films formed in this manner are usually acid-catalyzed and thus have a compact structure with low porosity. As discussed previously, base-catalyzed sol–gels are usually of higher porosity, a critical issue in many sol–gel sensing applications. A promising method that has recently emerged for the formation of sol–gel films of high porosity is the electrodeposition of sol–gels at electrode surfaces.[17–19] This technique relies on the application of a negative potential to increase the pH at the electrode surface through the generation of OH^- ions, causing the immediate sol–gel condensation. The unique aspect of this procedure is that gelation and drying proceed independently of each other, allowing for the formation of films with greater porosity.[17]

With this electrodeposition technique, a pyridine-functionalized sol–gel film was deposited at the surface of a glassy carbon electrode. When this modified electrode was exposed to a Cr(VI)-containing solution, preconcentration similar to that using the pyridine-functionalized monoliths occurred; the positively-charged pyridinium groups interacted with the negatively-charged Cr(VI) anions. Square-wave voltammograms were used for the analysis of varying Cr(VI) concentrations (Figure 5), and a linear relationship between the peak current, generated at the functionalized electrode by the Cr(VI) to Cr(III) reduction and the Cr(VI) concentration in solution was
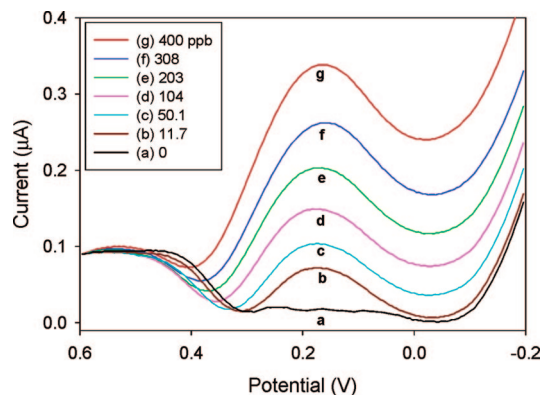
observed ($R = 0.996$). Concentrations as low as 4.6 ppb Cr(VI) could be determined, and the electrodes were found to demonstrate a high selectivity and reproducibility. Interference studies showed that a 10^5 excess of Cr(III) could be tolerated with no adverse effects to the peak current, and numerous other metal ions showed little or no interference. This selectivity for Cr(VI) is not surprising, because it is one of a few anionic metal species.

Development of such electrochemical and optical Cr(VI) sensors was motivated in part by the determination of chromium in biological fluids. Chromium at the +3 oxidation state is an essential trace element for mammals, and there is a need for its determination in biological samples.[32] The detection limits provided by the sol–gel Cr(VI) sensors described in this Account approach the typical chromium concentration in blood. However, analysis of biological chromium is not straightforward, because chromium is bound to biological and organic species, complicating its detection. Sample pretreatment is thus needed to remove these species. We have recently used the advanced oxidation process (AOP), a combination of H_2O_2 and UV irradiation to generate •OH radicals, to destroy organic matter in blood.[32] This process also oxidizes Cr(III) to Cr(VI) for subsequent electrochemical analysis.[32] Such a pretreatment procedure may also be applied to other inorganic sensing applications where the presence of ligands and organic matter may interfere with the analysis.[33]

6. Conclusions and Outlook

The studies discussed in this Account have demonstrated the versatility of sol–gels and the methods by which they may be employed in sensing applications. With numerous variables involved in the synthetic process, sol–gels can be specifically tailored to meet a variety of needs. Through the grafting and entrapping of organic molecules, these substrates can be modified to show specificity for analytes of interest. Such procedures can provide many types of sol–gel sensing substrates, from doped thin films to functionalized monoliths to electrodeposited coatings. This versatility makes sol–gels especially attractive for use in sensing applications. The design and preparation of

new sol–gel precursors containing grafted inorganic/organic functional groups would further broaden the selection of sol–gel sensors and their applications.

Although this Account highlights sol–gel use in optical and electrochemical sensors, their design and implementation is in no way limited to these sensing areas, since they have found use in spectroelectrochemical and mass-sensitive devices as well. In addition, sol–gel chemistry extends well beyond sensing boundaries, with sol–gels finding applications in separation techniques, catalysis, and a host of other areas. With their versatility and ease of functionality, it is certain that innovation in sol–gel preparation and use will continue into the future.

References

(1) Brinker, C. J.; Scherer, G. W. *Sol–Gel Science*; Academic Press: San Diego, CA, 1990.

(2) (a) Allain, L. R.; Sorasaenee, K.; Xue, Z. Doped thin-film sensors via a sol–gel process for high-acidity determination. *Anal. Chem.* **1997**, *69*, 3076–3080. (b) Allain, L. R.; Xue, Z. Optical sensors for the determination of concentrated hydroxide. *Anal. Chem.* **2000**, *72*, 1078–1083. (c) Allain, L. R.; Xue, Z. Hysteresis in optical sensing and its impact on the analytical error of a calibration-free acid sensor. *Anal. Chim. Acta* **2001**, *433*, 97–102.

(3) Schubert, U; Huesing, N.; Lorenz, A. Hybrid inorganic–organic materials by sol–gel processing of organofunctional metal alkoxides. *Chem. Mater.* **1995**, *7*, 2010–2027.

(4) (a) Carey, W. P.; Jorgensen, B. S. Optical sensors for high acidities based on fluorescent polymers. *Appl. Spectrosc.* **1991**, *45*, 834–838. (b) Carey, W. P.; DeGrandpre, M. D.; Jorgensen, B. S. Polymer-coated cylindrical waveguide absorption sensor for high acidities. *Anal. Chem.* **1989**, *61*, 1674–1678.

(5) Lev, O.; Tsionsky, M.; Rabinovich, L.; Glezer, V.; Sampath, S.; Pankratov, I.; Gun, J. Organically modified sol–gel sensors. *Anal. Chem.* **1995**, *67*, 22A–30A.

(6) (a) Klein, L. C. Sol-gel coatings. In *Coatings Technology Handbook*, 3rd ed.; Tracton, A. A., Ed.; CRC Press: Boca Raton, FL, 2006; pp 96/1–96/4. (b) Sanchez, C.; Julian, B.; Belleville, P.; Popall, M. Applications of hybrid organic–inorganic nanocomposites. *J. Mater. Chem.* **2005**, *15*, 3559–3592. (c) McDonagh, C.; MacCraith, B. D.; McEvoy, A. K. Tailoring of sol–gel films for optical sensing of oxygen in gas and aqueous phase. *Anal. Chem.* **1998**, *70*, 45–50.

(7) Lin, J.; Brown, C. W. Sol–gel glass as a matrix for chemical and biochemical sensing. *Trends Anal. Chem.* **1997**, *16*, 200–211.

(8) (a) MacCraith, B. D.; Ruddy, V.; Potter, C.; O'Kelly, B.; McGilp, J. F. Optical waveguide sensor using evanescent wave excitation of fluorescent dye in sol–gel glass. *Electron. Lett.* **1991**, *27*, 1247–1248. (b) Lobnik, A.; Oehme, I.; Murkovic, I.; Wolfbeis, O. S. pH optical sensors based on sol–gels. Chemical doping versus covalent immobilization. *Anal. Chim. Acta.* **1998**, *367*, 159–165.

(9) Avnir, D. Organic chemistry within ceramic matrixes: doped sol–gel materials. *Acc. Chem. Res.* **1995**, *28*, 328–334.

(10) (a) Dunn, B.; Zink, J. I. Optical properties of sol–gel glasses doped with organic molecules. *J. Mater. Chem.* **1991**, *1*, 903–913. (b) Lev, O. Diagnostic applications of organically-doped sol–gel porous glass. *Analusis* **1992**, *20*, 543–553.

(11) (a) Allain, L. R.; Canada, T. A.; Xue, Z. Optical sensors and the salt effect: A dual transducer approach to acidity determination in a salt-containing concentrated strong acid. *Anal. Chem.* **2001**, *73*, 4592–4598. (b) Canada, T. A.; Allain, L. R.; Beach, D. B.; Xue, Z. High-acidity determination in salt-containing acids by optical sensors. The scope of a dual-transducer approach and the Hammett acidity function. *Anal. Chem.* **2002**, *74*, 2535–2540.

(12) (a) Shamsipur, M.; Gholamhassan, A. High-acidity optical sensors based on sol–gel derived thin films. *Anal. Lett.* **2001**, *34*, 1603–1616. (b) Wang, E.; Chow, K.-F.; Wang, W.; Wong, C.; Yee, C.; Persad, A.; Mann, J.; Bocarsly, A. Optical sensing of HCl with phenol red doped sol–gels. *Anal. Chim. Acta* **2005**, *534*, 301–306.

(13) (a) Canada, T. A.; Xue, Z. High-basicity determination in mixed water–alcohol solutions by a dual optical sensor approach. *Anal. Chem.* **2002**, *74*, 6073–6079. (b) Canada, T. A.; Beach, D. B.; Xue, Z. Optical sensors for the determination of concentrated hydroxide. Characterization of the sensor materials and evaluation of the sensor performance. *Anal. Chem.* **2005**, *77*, 2842–2851.

(14) (a) Rodman, D. L.; Pan, H.; Clavier, C. W.; Feng, X.; Xue, Z. Optical metal ion sensor based on diffusion followed by an immobilizing reaction. Quantitative analysis by a mesoporous monolith containing functional groups. *Anal. Chem.* **2005**, *77*, 3231–3237. (b) Clavier, C. W.; Rodman, D. L.; Sinski, J. F.; Allain, L. R.; Im, H.-J.; Yang, Y.; Clark, C. J.; Xue, Z. A method for the preparation of transparent mesoporous silica sol–gel monoliths containing grafted organic functional groups. *J. Mater. Chem.* **2005**, *15*, 2356–2361. (c) Carrington, N. A.; Thomas, G. H.; Rodman, D. L.; Beach, D. B.; Xue, Z. Optical determination of Cr(VI) using regenerable, functionalized sol–gel monoliths. *Anal. Chim. Acta* **2007**, *581*, 232–240.

(15) (a) Zevin, M.; Reisfeld, R.; Oehme, I.; Wolfbeis, O. S. Sol–gel derived optical coatings for determination of chromate. *Sens. Actuators, B* **1997**, *B39*, 235–238. (b) Oehme, I.; Wolfbeis, O. S. Optical sensors for determination of heavy metal ions. *Mikrochim. Acta* **1997**, *126*, 177–192.

(16) See, for example, (a) Lan, E. H.; Dave, B. C.; Fukuto, J. M.; Dunn, B.; Zink, J. I.; Valentine, J. S. Synthesis of sol–gel encapsulated heme proteins with chemical sensing properties. *J. Mater. Chem.* **1999**, *9*, 45–53. (b) Narang, U.; Prasad, P. N.; Bright, F. V.; Ramanathan, K.; Kumar, N. D.; Malhotra, B. D.; Kamalasanan, M. N.; Chandra, S. Glucose biosensor based on a sol–gel-derived platform. *Anal. Chem.* **1994**, *66*, 3139–3144. (c) Wang, J. Sol–gel materials for electrochemical biosensors. *Anal. Chim. Acta* **1999**, *399*, 21–27. (d) Rao, M. S.; Dave, B. C. "Smart" glasses: Molecular programming of rapid dynamic responses in organosilica sol–gels. *Adv. Mater.* **2002**, *14*, 443–447.

(17) Deepa, P. N.; Kanungo, M.; Claycomb, G.; Sherwood, P. M. A.; Collinson, M.M. Electrochemically deposited sol–gel derived silicate films as a viable alternative in thin-film design. *Anal. Chem.* **2003**, *75*, 5399–5405.

(18) Walcarius, A.; Sibottier, E. Electrochemically-induced deposition of amine-functionalized silica films on gold electrodes and application to Cu(II) detection in (hydro)alcoholic medium. *Electroanal.* **2005**, *17*, 1716–1726.

(19) Shacham, R.; Avnir, D.; Mandler, D. Electrodeposition of methylated sol–gel films on conducting surfaces. *Adv. Mater.* **1999**, *11*, 384–388.

(20) (a) Walcarius, A.; Mandler, D.; Cox, J. A.; Collinson, M.; Lev, O. Exciting new directions in the intersection of functionalized sol–gel materials with electrochemistry. *J. Mater. Chem.* **2005**, *15*, 3663–3689. (b) Lev, O.; Wu, Z.; Bharathi, S.; Glezer, V.; Modestov, A.; Gun, J.; Rabinovich, L.; Sampath, S. Sol–gel materials in electrochemistry. *Chem. Mater.* **1997**, *9*, 2354–2375. (c) Alber, K. S.; Cox, J. A. Electrochemistry in solids prepared by sol–gel processes. *Mikrochim. Acta* **1997**, *127*, 131–147.

(21) (a) Carrington, N. A.; Yong, L.; Xue, Z. Electrochemical deposition of sol–gel films for enhanced chromium(VI) determination in aqueous solutions. *Anal. Chim. Acta* **2006**, *572*, 17–24. (b) Carrington, N.A.; Qiu, H.; Xue, Z. Electrodeposited sol–gels for electrochemical sensing of Cr(VI). Am. Lab. 2007, in press.

(22) Shi, Y.; Slaterbeck, A. F.; Seliskar, C.J.; Heineman, W. R. Spectroelectrochemical sensing based on multimode selectivity simultaneously achievable in a single device. 1. Demonstration of concept with ferricyanide. *Anal. Chem.* **1997**, *69*, 3679–3686.

(23) See, for example, (a) Yu, X.-H.; Morton, L.A.; Xue, Z.-L. Transition metal silyl complexes and chemistry in the reactions of silanes with transition metal complexes. *Organometallics* **2004**, *23*, 2210–2224. See, for example, (b) Yu, X.-H.; Cai, H.; Guzei, I.A.; Xue, Z.-L. Unusual equilibria involving Group 4 amides, silyl complexes, and silyl anions via ligand exchange reactions. *J. Am. Chem. Soc.* **2004**, *126*, 4472–4473.

(24) *Kirk-Othmer Encyclopedia of Chemical Technology*, 4th ed.; Wiley: New York, 1991; Vol. 1, pp 938–1025; 1995; Vol. 13, pp 894–925.

(25) Greenwood, N. N.; Earnshaw, A. *Chemistry of the Elements*, 2nd ed.; Pergamon Press: New York, 1997; p 89 and p 811.

(26) Bishop, E. *Indicators*; Pergamon Press: Oxford, U.K., 1972.

(27) Paul, A. Chemical durability of glasses; a thermodynamic approach. *J. Mater. Sci.* **1977**, *12*, 2246–2268.

(28) (a) Chow, E.; Gooding, J. J. Peptide modified electrodes as electrochemical metal ion sensors. *Electroanalysis* **2006**, *18*, 1437–1448. (b) Zanello, P. *Inorganic Electrochemistry: Theory, Practice and Applications*; Royal Society of Chemistry: Cambridge, U.K., 2003.

(29) Mansur, H. S.; Vasconcelos, W. L.; Lenza, R. S.; Orefice, R. L.; Reis, E. F.; Lobato, Z. P. Sol–gel silica based networks with controlled chemical properties. *J. Non-Cryst. Solids* **2000**, *273*, 109–115.

(30) Zhang, Y.; Ji, H.-F.; Brown, G. M.; Thundat, T. Detection of CrO_4^{2-} using a hydrogel swelling microcantilever sensor. *Anal. Chem.* **2003**, *75*, 4773–4777.

(31) Turyan, I.; Mandler, D. Selective determination of Cr(VI) by a self-assembled monolayer-based electrode. *Anal. Chem.* **1997**, *69*, 894–897.

(32) (a) Yong, L.; Armstrong, K. C.; Dansby-Sparks, R. N.; Carrington, N. A.; Chambers, J. Q.; Xue, Z.-L. Quantitative analysis of trace chromium in blood samples. Combination of the Advanced Oxidation Process with catalytic adsorptive stripping voltammetry. *Anal.* *Chem.* **2006**, *78*, 7582–7587. (b) Rodman, D. L.; Carrington, N. A.; Xue, Z.-L. Conversion of chromium(III) propionate to chromium(VI) by the Advanced Oxidation Process: Pretreatment of a biomimetic complex for metal analysis. *Talanta* **2006**, *70*, 668–675.

(33) Rodman, D. L.; Carrington, N. A.; Xue, Z.-L. Studies of the oxidation of palladium complexes by the Advanced Oxidation Process. Pretreatment of model catalysts for precious metal analysis. *Talanta* **2006**, *70*, 426–431.

AR600017W